

## Atomistic Study of Anomalous Self-Diffusion in bcc $\beta$ -Titanium

W. Petry, T. Flottmann,<sup>(a)</sup> A. Heiming, J. Trampenau, and M. Alba

*Institut Laue-Langevin, F-38042 Grenoble Cedex, France*

and

G. Vogl

*Institut für Festkörperphysik der Universität Wien, A-1090 Wien, Austria*

(Received 2 May 1988)

In an investigation of self-diffusion in bcc  $\beta$ -Ti single crystals by means of both quasielastic and inelastic neutron scattering, the elementary diffusion jump has been determined directly, and the lattice vibrations which trigger the jump have been elucidated. The elementary jump for self-diffusion is a simple  $\frac{1}{2}$  [111] jump into a nearest-neighbor vacancy. The reason for the anomalously fast self-diffusion is a fluctuation of  $\omega$ -phase type which facilitates jumps into neighboring vacancies.

PACS numbers: 66.30.Fq, 61.12.-q, 61.70.Bv, 63.20.Dj

Self-diffusion in the bcc high-temperature  $\beta$  phase of the metals Ti, Zr, and Hf (IVB group of the periodic system) is anomalous in two respects: (i) When normalized to the melting-point temperature, the diffusivities are several orders of magnitude higher than for other bcc metals.<sup>1</sup> (ii) The Arrhenius plots (i.e., logarithm of diffusivity versus reciprocal temperature) of  $\beta$ -Ti,  $\beta$ -Zr, and  $\beta$ -Hf are strongly curved whereas those for other bcc metals deviate only slightly from linearity.<sup>1</sup>

Numerous attempts have been made to explain anomalous diffusion in the IVB metals. Among these are (i) two diffusion mechanisms, i.e., diffusion via vacancies aided by diffusion via divacancies<sup>2</sup> or interstitials,<sup>3</sup> the latter mechanisms increasing in importance with increasing temperature; (ii) lattice anharmonicity around a monovacancy leading to temperature-dependent activation enthalpy<sup>4</sup>; (iii) destabilization of the lattice due to the tendency to form precursors of the low-temperature  $\alpha$  phase<sup>5</sup> or of the metastable  $\omega$  phase.<sup>1,6</sup>

These explanations are based on *indirect* experimental evidence. Here for the first time, we present a *direct* atomistic determination of the elementary diffusion jump and of the lattice vibrations triggering it, and we therefore are able to arrive at a self-consistent microscopic description of self-diffusion in the  $\beta$  phase of the IVB metals.

The methods applied in this study were incoherent quasielastic and coherent inelastic neutron scattering (QNS and INS). With incoherent QNS, very small energy transfers (in the range of 1  $\mu$ eV) from individual atoms to the neutrons or vice versa are measured as a function of transferred momentum. This corresponds to a determination of the energy uncertainty due to a noninfinite residence time  $\tau$  of an atom at one and the same lattice site. From the dependence of the energy broadening on transferred momentum and on crystal orientation all details of the atomic jump (jump vector, jump frequency) of an individual atom can be de-

duced.<sup>7-10</sup> We have used the backscattering spectrometer IN10 at the Institute Laue-Langevin for our studies.

With coherent INS, energy transfers from (to) the phonons to (from) the neutrons are studied, i.e., energy changes in the range of millielectronvolts. We have used the three-axis spectrometer IN8 at the Institute Laue-Langevin. As will be seen, INS permits us to learn about the lattice-dynamical causes of anomalous diffusion, namely, an extreme softening of the phonons at the so-called  $\omega$  point.

Of the three IVB metals we have chosen Ti, because compared to Zr and Hf it has the highest incoherent-neutron-scattering cross section ( $\sigma_{\text{inc,Ti}} = 2.7$  b,<sup>11</sup>  $\sigma_{\text{inc,Zr}} = 0.04$  b,<sup>12</sup>  $\sigma_{\text{inc,Hf}} = 2.6$  b<sup>11</sup>). Compared to Hf, it has a weak cross section for absorption and a considerably wider range of stability of the  $\beta$  phase. Polycrystalline Ti metal, in the form of rods, was supplied by MRC France [analysis by MRC: Cr, 20; Fe, 50; Ni, 30; Pb, 15; Sn, 20; C, 30; H, 2; analysis by Bundesanstalt für Materialforschung (BAM), Berlin: N, 97(7); O, 547(23), all figures in ppm by weight].

Since bcc  $\beta$ -Ti transforms via a martensitic phase transition at 882 °C to hcp  $\alpha$ -Ti, we had to develop a furnace which permits us to grow single crystals *in situ* and afterwards—without intermediate cooling down—serves as the measuring furnace. Details of the furnace and crystal growth by the floating-zone technique have been reported recently.<sup>13</sup> The crystals grown for the measurements reported here were about 5 cm long and 0.8 cm thick. Each of the measurement series—two on IN10 and one on IN8—lasted for about twelve days during which time the crystal was grown, oriented directly on the spectrometer, and kept at high temperatures. The grown crystals showed a good quality, i.e., rocking curves of different Bragg peaks never indicated a width larger than the IN8 resolution. Temperatures were 1460 and 1530 °C for the QNS measurements and 1020 °C for the INS studies. The temperatures were measured with a

two-color pyrometer. To reduce the background in the neutron scattering, we avoided the use of a heating element for the crystal and heating was achieved by sending a current directly through the sample. The inevitable temperature gradients were measured to be  $\pm 1\%$  of the indicated temperature over the heights of the neutron beam of 3 cm. The sample environment was vacuum (better than  $10^{-7}$  mbar) for the first QNS measurements and high-purity argon gas (pressure 100 mbar) for all other measurements. After the INS measurements the Ti was analyzed by BAM for gaseous impurities and an increase to 214(10) ppm by weight N and 1553(19) ppm by weight O was found.

Figure 1 shows the quasielastic energy broadening  $\Gamma$  at different temperatures for various crystal orientations as a function of the absolute value of the momentum transfer  $Q$ . According to Singwi and Sjölander<sup>14</sup> for the simplest case of random jumps between nearest-neighbor (NN) positions only, the energy broadening  $\Gamma$  is con-

nected to the jump frequency  $1/\tau$  and the jump vectors  $\mathbf{R}_n$  in the following way (compare Refs. 7 and 8):

$$\Gamma = \frac{2\hbar}{\tau} \left[ 1 - \frac{1}{N} \sum_{n=1}^N \exp(i\mathbf{Q} \cdot \mathbf{R}_n) \right]. \quad (1)$$

$n=1, \dots, N$  denotes the possible jump vectors starting from a given site.

Any realistic diffusion jump model has to include correlations between consecutive jumps through multiple exchange with one and the same point defect. Therefore, we may write<sup>15</sup>

$$\Gamma = \frac{2\hbar}{\tau_{\text{enc}}} \left[ 1 - \sum_{n=1}^N W_n \exp(i\mathbf{Q} \cdot \mathbf{R}_n) \right], \quad (2)$$

where a single NN jump has been replaced by the sum over all displacements of a given atom caused by a point defect.  $\tau_{\text{enc}}$  refers to the mean time between two encounters and the sum extends to all  $N$  jump vectors  $\mathbf{R}_n$  which can be achieved during one encounter, weighted by their probability  $W_n$ . In Fig. 1 the measured data are compared with various model calculations that we have performed on the basis of Eq. (2). For NN and NNN (next-nearest-neighbor) jumps into vacancies, correlations between consecutive jumps have been taken into account via Monte Carlo simulations with a computer program originally due to Wolf.<sup>9,15</sup> Jumps on octahedral or tetrahedral interstitial sites show no correlation—the interstitial lattice is considered to be an empty lattice. Because the interstitial sites do not form a Bravais lattice, the  $m$  inequivalent sites per unit cell ( $m=4$  and  $3$  for tetrahedral and octahedral sites, respectively) give rise to  $m$  Lorentzians with different line broadenings  $\Gamma_m$ . For simplicity the different  $\Gamma_m$  have been averaged to one effective linewidth shown in Fig. 1. Similar calculations have been performed earlier by Rowe *et al.*<sup>16</sup>

The various models have been fitted simultaneously to all crystal orientations of each measuring series, thus leaving only one fit parameter  $\tau_{\text{enc}}$  for each of the two different temperatures. From that we have finally deduced the tracer diffusivity  $D$  via the Einstein-Smoluchowski equation  $D = d^2 f / 6\tau$ . Here  $d$  is the length of an elementary jump (not the length of an encounter) and  $1/\tau$  is the jump frequency which is related to  $\tau_{\text{enc}} = z_{\text{enc}} \tau$  via the average number of jumps  $z_{\text{enc}}$  during one encounter.  $f$  is the macroscopic correlation factor; values for  $\tau_{\text{enc}}$  and  $f$  can be extracted from the Monte Carlo simulations.<sup>9,15</sup> Table I summarizes our results and compares them with diffusivities measured from tracer studies.  $\chi^2$  has been included as a measure of the quality of the fits. From Fig. 1 it is evident that the model calculations for NN jumps fit the data much better than the various other models (see also  $\chi^2$  in Table I).

A further criterion for the validity of a jump model is that the diffusion coefficients deduced from QNS can be compared with those measured by tracer techniques.

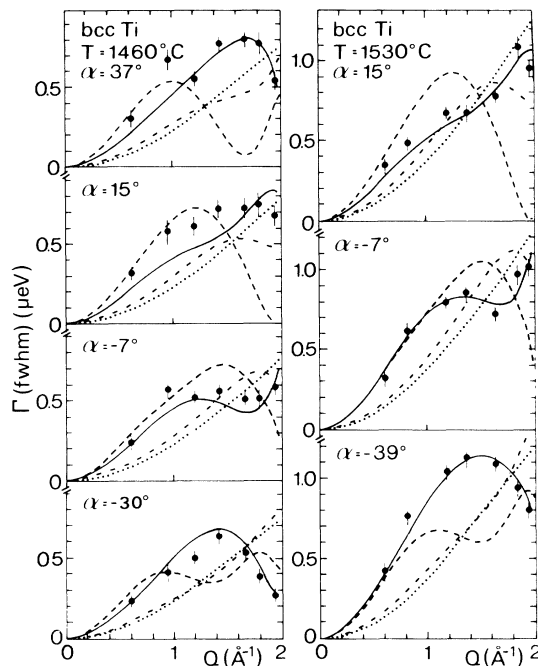


FIG. 1. Measured quasielastic line broadening  $\Gamma(Q)$  for two measuring series of bcc Ti at 1460°C (left) and 1530°C (right) as a function of scattering vector  $Q$ , with respect to the lattice orientation. Left: scattering plane parallel to the (001) crystal plane. Right: scattering plane parallel to the (012) crystal plane.  $\alpha$  denotes a rotation of the sample around an axis perpendicular to the scattering plane and is defined as the angle between incident neutrons and the  $\langle 100 \rangle$  crystal direction (clockwise). Because IN10 is a multidetector instrument, the  $Q$  axis corresponds to half an Ewald circle in reciprocal space with a diameter of  $2.0 \text{ \AA}^{-1}$ . Comparison with model calculations: solid line,  $\frac{1}{2} [111]$  NN jumps; dashed line,  $[100]$  NNN jumps; dotted line, tetrahedral interstitial jumps; dash-dotted line, octahedral interstitial jumps.

TABLE I. Results of model calculations and corresponding fits to the data (see text); comparison with measured tracer diffusivity.

Jump model	$f$	$z_{enc}$	$\chi^2$	$T=1460^\circ\text{C}$		$T=1530^\circ\text{C}$	
				$10^{12}D$ (m <sup>2</sup> /sec)	$\chi^2$	$10^{12}D$ (m <sup>2</sup> /sec)	$\chi^2$
Tetrahedral sites	...	...	21.1	1.9	33.2	3.1	
Octahedral sites	...	...	21.9	2.5	31.2	3.9	
NNN position	0.653	1.47	23.2	9.1	49.9	10.8	
NN position	0.727	1.36	2.96	5.4	1.70	8.9	
Tracer diffusivities <sup>a</sup>				7.9		12.9	

<sup>a</sup>Taken from Ref. 1 and references therein.

Table I indicates that the diffusivities deduced from the NN model are roughly 30% below the tracer data. The diffusivities deduced from the NNN model show a better agreement. Whereas  $\chi^2$  directly indicates that a NNN model alone has to be excluded, an admixture of NNN jumps to the dominating NN jumps (beyond that which is already included in the correlation) has to be considered.<sup>17</sup> Indeed, if we take the data measured at 1460°C, an admixture of up to 25% NNN jumps still gives reasonable fit results.<sup>18</sup> The more extensive measurements at higher temperatures, however, show a significant increase in  $\chi^2$  when we admit any admixture of NNN jumps, even though we should expect at these high temperatures a relative increase in the divacancy concentration and therefore most probably an increase of the NNN jump admixture. Consequently, we conclude that a NNN jump contribution has to be considerably below 25%. The discrepancy in the diffusion constants remains an open problem and will be discussed in a forthcoming paper.

Having thus shown that self-diffusion is dominated by

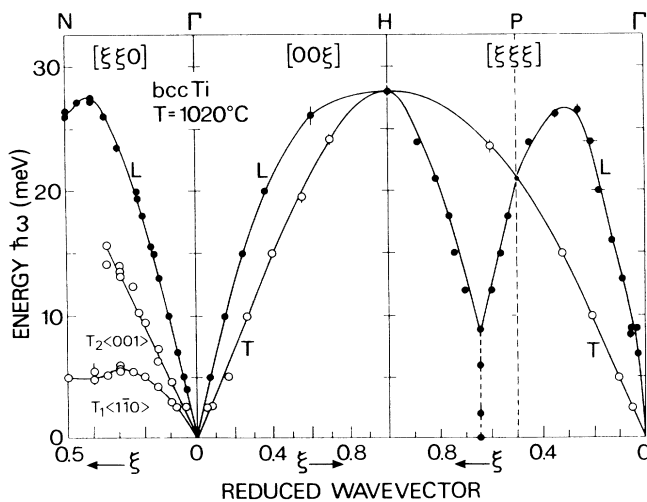


FIG. 2. Phonon dispersion of bcc Ti along the  $[\xi\xi0]$ ,  $[00\xi]$ , and  $[\xi\xi\xi]$  symmetry directions at 1020°C. The solid lines were drawn as guides to the eye only.

$\frac{1}{2} [111]$  jumps into NN vacancies, we are left with the question of why these jumps are so frequent. To shed more light onto this problem we have studied for the first time lattice vibrations in  $\beta$ -Ti.

Inelastic-neutron-scattering studies by Stassis and co-workers<sup>19</sup> have shown that in  $\beta$ -Zr a phenomenon known for all bcc metals becomes particularly striking, i.e., the softening of the longitudinal (L)  $[\xi\xi\xi]$  vibrational mode at  $\mathbf{q} = \frac{2}{3} (1,1,1)$ . Sanchez and DeFontaine<sup>6</sup> and recently Herzig and Köhler<sup>1</sup> have argued that it is exactly this low-energy mode which freezes into quasistatic displacements of the bcc lattice towards the  $\omega$  phase. The connection with diffusion is clear since these displacements have the configuration of the first saddle point or activated complex for diffusion in bcc structures, provided the diffusion happens via NN vacancies; i.e., lattice instabilities towards the  $\omega$  phase reduce the activation energy for jumps into NN vacancies. Recently, Herzig and Köhler<sup>1</sup> have argued that all bcc metals show a more or less pro-

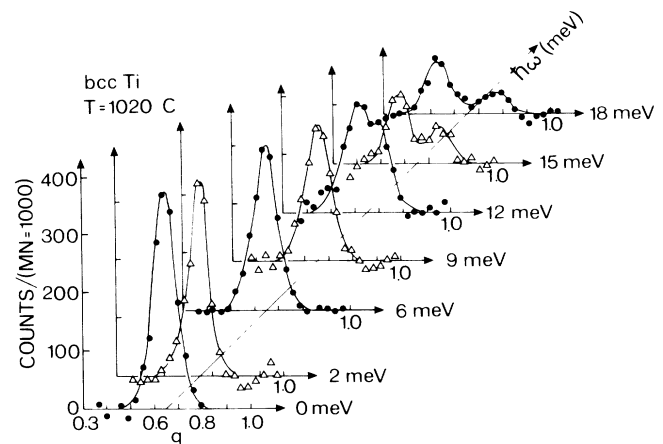


FIG. 3. Constant-energy scans along  $\mathbf{q}||[\xi\xi\xi]$  for different neutron energy losses  $\hbar\omega$ . The neutron counts are background corrected and normalized to a monitor count of 1000. For  $\hbar\omega=0$  meV, the measured incoherent scattering has been subtracted. The solid lines represent fits with one or two Gaussians of almost constant width (FWHM) of 0.10 radiation length.

nounced dip in the L  $[\xi\xi\xi]$  phonon branch and therefore the above considerations are—to some extent—valid for all bcc metals. We have therefore decided to thoroughly study this phenomenon for  $\beta$ -Ti.

For the quasielastic scattering sufficiently high temperatures had been chosen in order to induce a sufficiently large line broadening. For inelastic scattering we chose a lower temperature in order to facilitate detection of the consequences of incipient low-temperature phases. Figure 2 shows the phonon dispersion measured on  $\beta$ -Ti. The most striking feature of the curves is the soft-mode behavior of the longitudinal  $[\xi\xi\xi]$  vibrational mode at  $q \approx \frac{2}{3}(1,1,1)$ . Another interesting feature—which will not be discussed in this Letter—is the extraordinary low frequency of one of the transverse (T)  $[\xi\xi0]$  zone-boundary phonons. The soft-mode behavior of the L  $\frac{2}{3}[111]$  mode has already been found by Stassis and Zarestky<sup>19</sup> for  $\beta$ -Zr and therefore is not surprising in itself. Interesting and new, however, are two points: (i) the soft mode reaches down to energy  $\hbar\omega=0$ , and (ii) there is *no* coherent elastic intensity at  $\hbar\omega=0$ . This is clearly indicated by Fig. 3 where constant-energy scans up to 18 meV are shown. At  $q = \frac{2}{3}(1,1,1)$  the energy distribution can be fitted by a damped oscillator centered at  $\hbar\omega=10$  meV with a width of 12 meV. The absence of coherent elastic intensity for the L  $\frac{2}{3}[111]$  at  $\hbar\omega=0$  is different from the  $\beta$ -Zr results of Stassis and Zarestky who found a strong elastic peak close to  $\frac{4}{3}\{1,1,1\}$ . They concluded that the low  $\frac{2}{3}[111]$  phonon freezes out into stable displacements towards the  $\omega$  phase, giving rise to a superstructure peak. Stassis and Zarestky, however, admitted that the high oxygen contamination (13000 and 2900 ppm by weight) of the samples might have been responsible for it. Our negative result now permits us to deduce more details about the tendency of the IVb metals to form the  $\omega$  phase. The nonexistence of a superstructure excludes the existence of static embryos of the  $\omega$  phase. The soft mode at  $\frac{2}{3}(1,1,1)$  with its large energy distribution down to  $\hbar\omega=0$  implies that short-lived phonons of the  $\omega$  type are formed; their lifetime follows from the energy width of the damped harmonic oscillator,  $\tau \approx 10^{-13}$  sec.

We have, therefore, the following self-consistent picture of self-diffusion in  $\beta$ -Ti (and most probably also in  $\beta$ -Zr and  $\beta$ -Hf). Diffusion occurs almost exclusively by atomic jumps into nearest-neighbor vacancies. These jumps are facilitated here compared to other bcc metals by the extreme tendency of the lattice to fluctuate in the direction of an  $\omega$ -phase structure without completing a phase transformation.

Financial support by Bundesministerium für Forschung und Technologie, Germany, under Project No.

03-ST1SPH-3 is gratefully acknowledged. We thank C. Herzig for discussions, and B. Dorner and R. Currat for advice in the interpretation of phonons.

<sup>(a)</sup>Now at AKZO Research Laboratories, D-8753 Obernburg, West Germany.

<sup>1</sup>C. Herzig and U. Köhler, *Mater. Sci. Forum* **15-18**, 301 (1987).

<sup>2</sup>A. Seeger and H. Mehrer, in *Vacancies and Interstitials in Metals*, edited by A. Seeger, D. Schumacher, W. Schilling, and J. Diehl (North-Holland, Amsterdam, 1970), p. 1.

<sup>3</sup>R. W. Siegel, in *Point Defects and Defect Interactions*, edited by J. Takamura, M. Doyama, and M. Kiritani (Tokyo Univ. Press, Tokyo, 1983), p. 533; R. W. Siegel, J. N. Mundy, and L. C. Smedskjaer, *Mater. Sci. Forum* **15-18**, 451 (1987).

<sup>4</sup>H. M. Gilder and D. Lazarus, *Phys. Rev. B* **18**, 4916 (1975); P. A. Varotsos, W. Ludwig, and K. D. Alexopoulos, *Phys. Rev. B* **18**, 2683 (1978).

<sup>5</sup>H. I. Aaronson and P. G. Shewmon, *Acta Metall.* **15**, 385 (1967).

<sup>6</sup>J. M. Sanchez and D. DeFontaine, *Phys. Rev. Lett.* **35**, 227 (1975), and *Acta Metall.* **26**, 1083 (1978); J. M. Sanchez, *Philos. Mag.* **43**, 1407 (1981).

<sup>7</sup>T. Springer, *Quasielastic Neutron Scattering for the Investigation of Diffusive Motions in Solids and Liquids*, Springer Tracts in Modern Physics Vol. 64, edited by G. Höhler (Springer-Verlag, Berlin, 1972).

<sup>8</sup>W. Petry and G. Vogl, *Mater. Sci. Forum* **15-18**, 323 (1987).

<sup>9</sup>G. Göltz, A. Heidemann, H. Mehrer, A. Seeger, and D. Wolf, *Philos. Mag. A* **41**, 723 (1980).

<sup>10</sup>M. Ait Salem, T. Springer, A. Heidemann, and B. Alefeld, *Philos. Mag. A* **39**, 797 (1979).

<sup>11</sup>V. F. Sears, Chalk River Nuclear Laboratory Report No. AECL-8490, 1984 (unpublished).

<sup>12</sup>W. Petry, G. Vogl, A. Heidemann, and K.-H. Steinmetz, *Philos. Mag. A* **55**, 183 (1987).

<sup>13</sup>T. Flottmann, W. Perry, R. Serve, and G. Vogl, *Nucl. Instrum. Methods A* **260**, 165 (1987).

<sup>14</sup>C. T. Singwi and A. Sjölander, *Phys. Rev.* **119**, 863 (1960), and **120**, 1093 (1960).

<sup>15</sup>D. Wolf, *Solid State Commun.* **23**, 853 (1977), and *Philos. Mag. A* **47**, 147 (1983).

<sup>16</sup>J. M. Rowe, K. Sköld, H. E. Flotow, and J. J. Rush, *J. Phys. Chem. Solids* **32**, 41 (1971).

<sup>17</sup>Significant admixtures of interstitial jumps can be excluded. Because of their jump length being small, the calculated  $\Gamma(\mathbf{Q})$  always shows a hump at large  $\mathbf{Q}$ , which is in complete disagreement with the experiment.

<sup>18</sup>T. Flottmann, W. Petry, G. Vogl, and A. Heiming, *Mater. Sci. Forum* **15-18**, 463 (1987).

<sup>19</sup>C. Stassis, J. Zarestky, and N. Wakabayashi, *Phys. Rev. Lett.* **41**, 1726 (1978); C. Stassis and J. Zarestky, *Solid State Commun.* **52**, 9 (1984).